SEMARAK ILMU PUBLISHING

Journal of Advanced Research in Fluid Mechanics and Thermal Sciences

Journal homepage:
https://semarakilmu.com.my/journals/index.php/fluid_mechanics_thermal_sciences/index
ISSN: 2289-7879

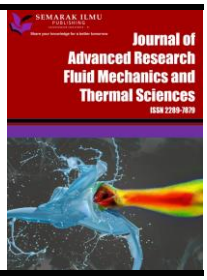

Control of Base Pressure at Supersonic Mach Number in a Suddenly Expanded Flow

Tun Nurhanis[1], Ambareen Khan[2], Mohammad Nishat Akhtar[2], Sher Afghan Khan[1,*]

[1] Department of Mechanical Engineering, Kulliyyah of Engineering, International Islamic University Malaysia, Malaysia
[2] School of Aerospace Engineering, Universiti Sains Malaysia, Nibong Tebal, Penang, Malaysia

ARTICLE INFO

Article history:
Received 8 June 2023
Received in revised form 17 August 2023
Accepted 28 August 2023
Available online 15 September 2023

Keywords:
Base pressure control; cavity; supersonic

ABSTRACT

In improving the efficiency of applications for flow over a blunt body like missiles and rockets, passive and active control is used to increase the base pressure, hence reducing the base drag. It must be mentioned that this paper covers mainly a variety of passive control methods in the form of the cavity, rib, splitter plate, spike, and some others to regulate the base pressure and drag force. Later, this paper focuses on the control of base pressure in the form of the cavity at a Mach number of 2.2 and an area ratio of 4.84. In this experiment, Computational Fluid Dynamics (CFD) is used to model a convergent-divergent nozzle and a duct. The cavity's dimensions and locations are studied to get the optimum cavity's control of base pressure. Two sizes of the cavity are considered which are 3:3 and 6:3. The L/D is varied from 1, 2, 4, and 6 while the Nozzle Pressure Ratio (NPR) ranges from 3 to 16. The 2-D design of a convergent-divergent axisymmetric nozzle suddenly expanded into a duct with a diameter of 22 mm with and without annular rectangular cavities is sketched using ANSYS. The results show that the base pressure is greatly influenced by the cavity's dimension and location as well as the NPR.

1. Introduction

The design and technological advancements of vehicles are evolving quickly over time. To guarantee that the vehicle created will be more efficient than before, both sectors necessitate considerable research. Drag can cause flow across a body to be interrupted, which will reduce the performance of the transportation for all vehicles. A vital analysis of base pressure in a suddenly expanded flow must be taken into account to ensure the effectiveness of an aerodynamic vehicle's functioning. The components of drag comprise skin friction drag and base drag. Moreover, for a supersonic Mach number, there is an additional component which is the wave drag that results from the shock that appeared. In supersonic flow, base drag which contributes 60 to 70 percent of the total drag is caused by the low-pressure region on the base of the object due to the flow separation of the fluid. When a body's height suddenly changes, the flow separates, and a region where the flow

* *Corresponding author.*
E-mail address: sakhan@iium.edu.my

https://doi.org/10.37934/arfmts.109.1.210225

is cycling creates a low-pressure area before the flow is reattached. The base drag is the only drag component that can be controlled by the design of the body of an object.

Generally, there are two ways to reduce the base drag; active and passive control. Active control requires an external source of energy which is undesirable in many aerospace vehicles as it will increase the weight. The only favorable option found in this type of control is the ability to turn on and off. Meanwhile, passive control is referred to when the device does not require any external energy to work on. The implementation of passive control systems can be done by modifying the shape and length of the device as well as adding additional structure to the device. Since the report's main emphasis is on passive control devices, some of them will be discussed in more detail which later will narrow the focus on the effect of the cavity.

The purpose of this study is to control the base pressure at supersonic Mach number in a suddenly expanded flow using passive control. The main goal of this study is to determine the best passive control device to regulate the base pressure that will eventually reduce the base drag. Moreover, the passive control in terms of the cavity is critically studied specifically, the effect of its dimension and location towards the base drag at supersonic Mach number. This study is also intended to improve the aerodynamic design of anybody who experiences the flow of air over it.

2. Literature Review

2.1 Cavity

The cavity is used to disrupt the flow and reduce the base drag by increasing the base pressure. The axisymmetric C-D nozzle connected to a circular duct and an annular rectangular cavity is shown in Figure 1.

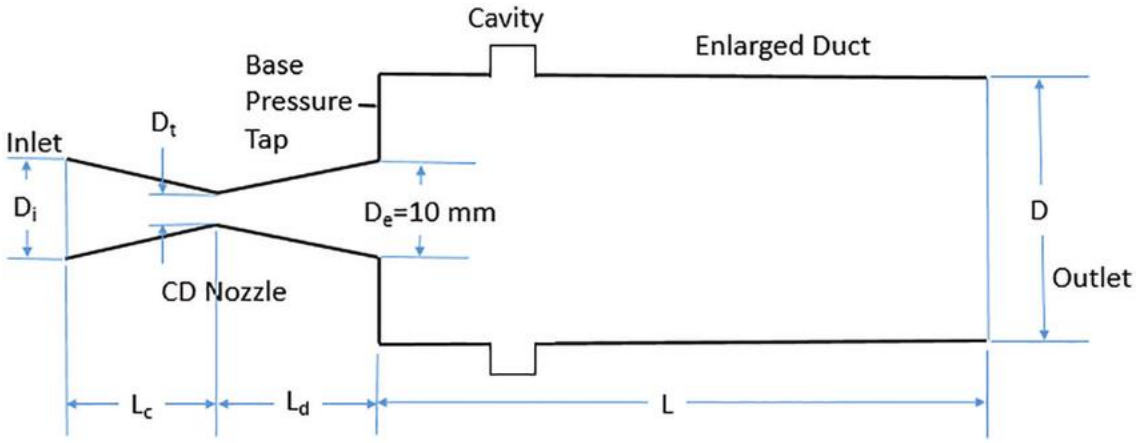

Fig. 1. Converging-diverging nozzle with suddenly expanded duct with an annular rectangular cavity

At the exit area of the nozzle, a low-pressure region appears due to the primary vortex that existed from the flow separation between the free shear layer, base wall, and reattachment point [1]. The presence of a cavity as a passive controller in the flow results in the formation of secondary vortexes. The interaction between these secondary vortexes and the primary vortex leads to an increase in base pressure [2]. The formation of the primary vortex and secondary vortex can be seen in Figure 2.

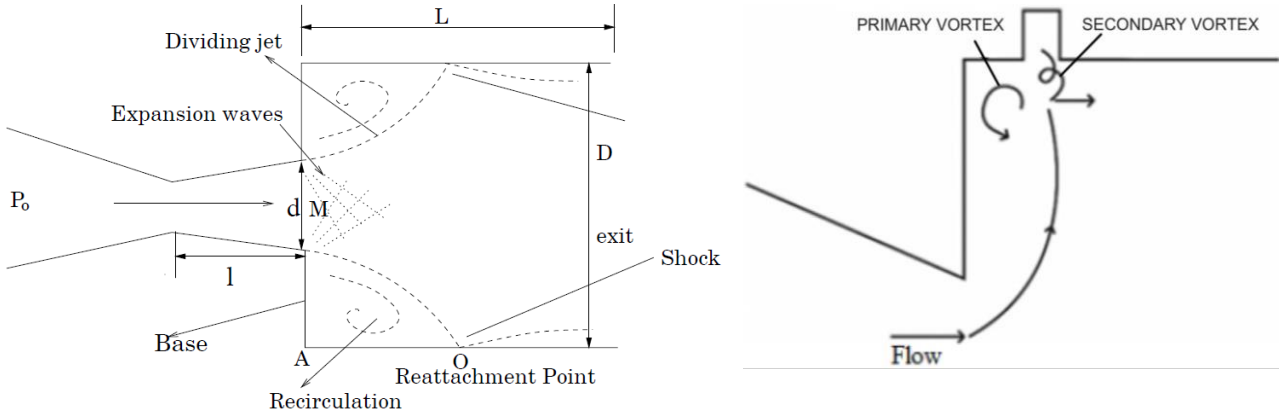

(a) (b)

Fig. 2. (a) Sudden expansion phenomenon (b) Interaction between primary and secondary vortex

There are two categories of cavities: open cavities and closed cavities. This group depends on the aspect ratio, sometimes known as the width-to-depth ratio, W/D. For an open cavity, the W/D is less than 10 while for a closed cavity, the aspect ratio is more than 12. Meanwhile, W/D lies in between and is called a transitional cavity. The location and dimension of the cavity should be at an optimum to successfully control the base drag.

2.2 Rib

When a cavity begins to act as a "closed cavity," which reduces its passive control effectiveness, a rib is introduced (Figure 3). The rib is positioned strategically to prevent the flow from reconnecting with the boundary layer in the base area. Unlike cavities, ribs are projections that create secondary vortices, which are expected to result in favorable base pressure values and an improved distribution of wall pressure [2].

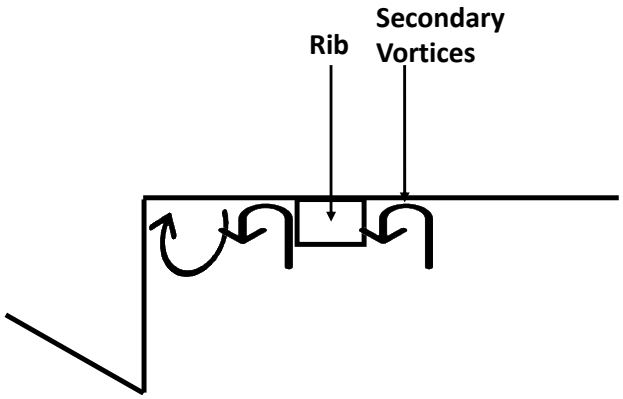

Fig. 3. Rib as a passive control

To optimize the use of ribs, various angles and shapes of the rib can be altered. One of the rib shapes is an isosceles right triangle that will cause an additional loss of energy. This energy will raise the average friction factor and decrease the Reynolds number because of the laminar sublayer. A secondary flow will develop close to the triangle's tip. Based on the findings of Rathakrishnan [3], a rib with a 3:1 ratio is the most effective in lowering the base drag as compared to 3:2 and 3:3. According to the same paper, the flow in the duct oscillates as the duct length is increased when ribs are used as passive controllers in abrupt expansion. The differences in base and wall pressure along

the duct must therefore be viewed as functions of different geometrical and flow characteristics. Passive control in the form of a rib plays an important role at a 3D/4D location, as Viswanath [4] explained. However, it lowers the ground pressure when placed at 1D. Here, we employ a 3mm wide rib ranging from 1mm to 4mm.

A numerical simulation was performed by Aabid *et al.,* [5] for a duct diameter of 20 mm and a rib with a height of 1 to 3 mm and a width of 3 mm at locations 1D, 2D, 3D, and 4D. It can be seen that the base pressure is higher with a rib case near the reattachment point than without one, regardless of height. In an experimental study using convolutional neural network predictions, Zuraidi *et al.,* [6] discovered that the rib cannot demonstrate its influence if the area ratio is high. According to experimental and numerical research on an area ratio of 7.84 using passive control in the form of a rib at sonic Mach number, the flow separation in the sudden expansion will affect the flow field [7].

2.3 Spikes

Spikes are commonly employed in the aerodynamic design of missiles and supersonic planes due to their ability to significantly reduce drag, temperature, and fuel consumption. When a blunt body moves through supersonic flow, it generates a high level of drag, resulting in the formation of shockwaves. These shockwaves cause increased pressure and temperature in the body. Four spikes of the body with different angles of the conical nose have been compared (Table 1) [10]. Figure 4 shows the comparison where Spike 4 gives the lowest drag coefficient.

Table 1
Different spikes used in the experiment

Spikes Body	Angles of the conical nose,˚
Without spike	-
Spike 1	20
Spike 2	5
Spike 3	10
Spike 4	Hemispherical

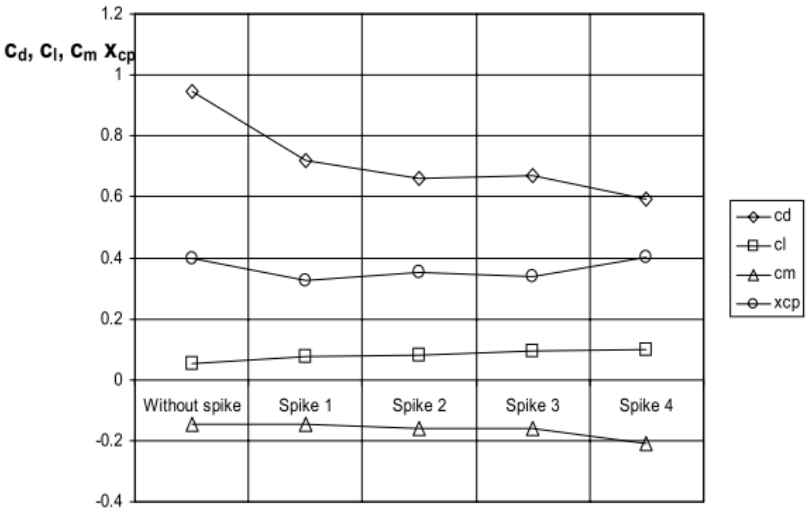

Fig. 4. Aerodynamics parameters obtained for different spikes 2.5

Other passive control methods, such as boat-tailing, can be utilized to manage base pressure. Boat-tailing involves encircling the end of a bluff body with a converging duct. This duct collects the free-stream flow and generates a high-speed jet resembling a boattail, directed towards the middle

of the bluff body's base surface. Khan *et al.,* [11] experimented using numerical large eddy simulation to study the effect of a jet boattail on bluff body models. The results showed a significant reduction in drag by increasing the base pressure and reducing the wake velocity deficit. The Large Eddy Simulation demonstrated a substantial 15% decrease in drag.

One of the passive control techniques that can be used for base pressure management is multistep afterbodies, as shown in Figure 5. Even though it is less effective than boat-tailing, it is still preferable to a blunt base that has not been changed. The base drag is lowered to 25–50% of drag reduction with a correct design compared to an unaltered base in research evaluating the effect of multistep after bodies [4]. Dimples are used to passively control the base pressure and reduce drag in the opposite direction [12]. The best L/D for a particular nozzle-pressure ratio can be found, and dimples can be used as a passive control to efficiently control drag. Experimental research into multiple cavities revealed their efficacy in lowering overall drag [13].

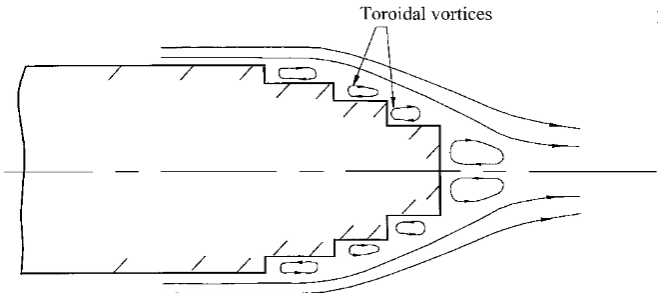

Fig. 5. Sketch of multistep after bodies

The cavity is one of the effective passive controls as it can be manipulated in many ways such as its dimensions and locations. A lot of studies can be found regarding cavities and the main working principle is to form a secondary vortex that will collide with the primary vortex to increase the base pressure and reduce the drag. In the next chapters, this paper will examine the effect cavity's dimension and location in regulating the base pressure.

2.6 Active Control

At Mach 1.5, the wall pressure is investigated while active control is used [14]. It was discovered that using the tiny jets as an active control had no negative effects on the flowfield. The simulation for the active control at supersonic Mach number was carried out using Computational Fluid Dynamics (CFD) software [15]. The results indicate that by controlling the base pressure, micro-jets are a viable technique for reducing total drag with little efficiency loss. In experimental studies of convergent-divergent nozzles, micro-jets are utilized for active control [16]. It was discovered throughout this study that micro-jets do not worsen the flowfield. Through the use of computational fluid dynamics and experimental design, micro-jets as active controls are investigated [17]. The analysis findings show that the L/D ratio is essential to the overall management of the system. Sajali *et al.,* [18] investigated how drag is impacted by the flow around the non-circular cylinder. Low pressure is located at the back and sides, whereas high and favorable pressure is present at the front. The only bodies that have such a high drag coefficient are bluff bodies with sharp turns. At Mach numbers between 0.3 and 3, computational fluid dynamics is utilized to study rapidly expanded flows both internally and externally [19]. In the fundamental region, it is discovered that internal and external rapidly enlarged flows have almost identical flow fields. Fluid dynamics analysis, both experimental and computer, is used to evaluate the nozzle-pressure ratio. At a nozzle pressure ratio of 8, microjets have been demonstrated to enhance the base pressure by 160–400% [20]. The

experimental examination of area ratios of 2.56, 3.24, 4.84, and 6.25 at Mach numbers between 1.6 and 2.0 showed that the influence of micro-jets at lower Mach numbers and area ratios is relatively minimal, but the micro-jets result in an increase of base pressure at all Mach numbers [21]. The minimal duct length for the flow to stay attached is 2D for nozzle pressure ratios greater than 5, according to research on convergent-divergent nozzles utilizing microjets at Mach 2.1 [22]. Shamitha *et al.,* [23] examined the wedge's surface pressure for a large angle of incidence at hypersonic Mach number. According to the findings, surface pressure increases as hypersonic Mach numbers and angle of incidence increase. Pathan *et al.,* [24] studied numerically the effectiveness of base pressure and reattachment length. According to the results, the nozzle becomes under-expanded with increased NPR, the reattachment length is decreased, and the base pressure tends to decrease at all the parameters of the current study. A study conducted by Pathan *et al.,* [25] concluded that base pressure and thrust are dependent variables and are functions of Mach number, NPR, area ratio, and L/D. Shaikh *et al.,* [26] studied the three-way catalytic converter and found that the overall pressure drop augments with velocity. Another study reported by Shaikh *et al.,* [27] provides information on the recirculation zones that were built into the base, along with velocity and pressure plots that were used to develop a solution for uniform flow inside the monolith and achieve a 3.7 Pa reduction in pressure drop.

3. Methodology

3.1 CD Nozzle Design

This section explains the process used to develop and model the nozzle. To ensure the correctness of the results, a 2-D Finite Element model that generated fine mesh is used. The analysis and the boundary conditions are also displayed.

The complete finite volume method (FVM) procedure was carried out using commercial software from Ansys called ANSYS Workbench, which is based on fluid flow (fluent) analysis systems. A concentrated axisymmetric duct with circular rectangular chambers is coupled to an axisymmetric convergent-divergent nozzle model in Figure 6. The model used is the same as previous experimental work by Pandey and Rathakrishnan [1]. The dimensions used are as depicted in Table 2 following the suitability with the Mach number of 2.2 for this study.

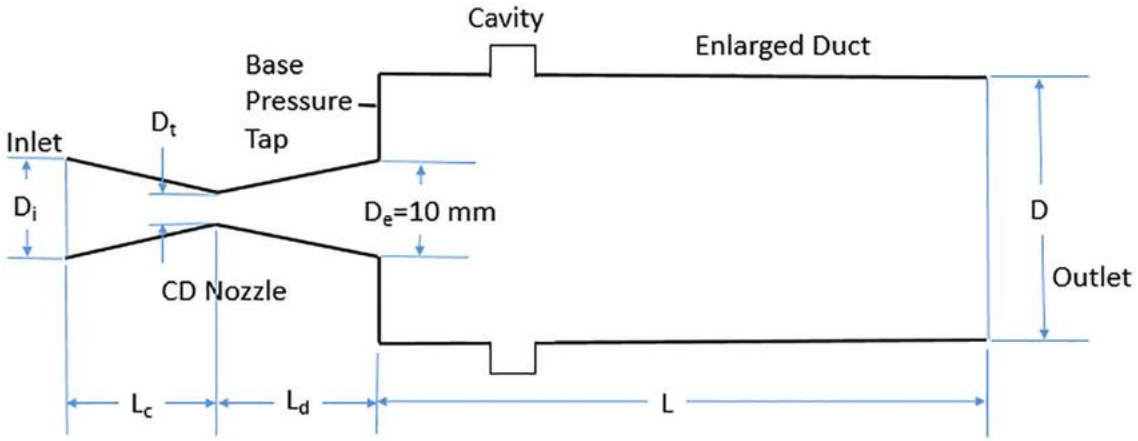

Fig. 6. CD nozzle model with duct and annular cavity (Pandey and Rathakrishnan [1])

Table 2
Dimensions of CD nozzle

Item	Value
Mach Number	1.74
Inlet diameter	26 mm
Outlet diameter	10 mm
Throat diameter	8.52 mm
Convergent length	17 mm
Cavity width	3 mm
Cavity depth	3 mm
Taping distance	3 mm
Duct diameter	17 mm
Duct length	Depends on the L/D ratio

3.2 Meshing

After sketching in the Design Modeler, the model needs to be generated before proceeding to mesh. The meshing process begins when the Automatic Method is used then it is applied to all quads. The element size is standardized to all dimensions of the CD nozzle which is 0.001 m element size (Figure 7).

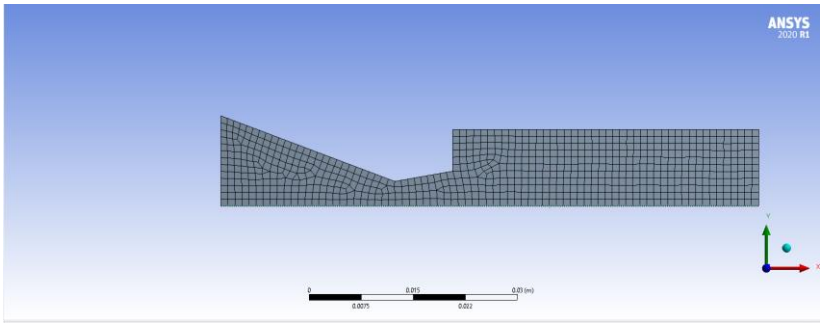

Fig. 7. Mesh density with an element size of 0.001m for L/D 2

3.3 CFD Simulation Setup

In the setup of a Computational Fluid Dynamics (CFD) simulation, various preparations are required before starting the calculation. These preparations include configuring general settings, models, materials, boundary conditions, initialization, and the calculation itself. In the general section, the solver type is set to density-based, and the simulation is set to steady-state. For a 2D analysis, the axisymmetric option is selected to solve the 2D axisymmetric problem.

The energy equation is chosen for the compressible flow, considering heat transfer and turbulent velocity [3]. The standard model uses k-epsilon (2 eqn) and Standard wall functions for near-wall treatment. Realizable and Scalable Wall Functions are selected for error calculation in some NPR experiments.

In the materials section, the simulation used fluid air, Sutherland law for viscosity, and constant values for molecular weight, thermal conductivity, and specific heat. Ideal gas density and properties were determined. The boundary conditions are set depending on the NPR which ranges from 3 to 16. Calculation and initialization are the final steps in this simulation setup. Hybrid initialization is chosen. The calculation is taken until 5000 iterations.

4. Results

4.1 Validation

This chapter validates the geometry of a C-D nozzle expanding into a circular duct with control using data from Pandey and Rathakrishnan's experiments. The experimental study by Pandey and Rathakrishnan [1] is conducted at Mach Number 1.74, NPR of 2.10, 2.65, 2.93, and 3.48, area ratios of 10, 6, and 2.89, and L/D ranging from 1 to 10. Figure 8 with NPR (P01/Pa) 2.65 from Pandey and Rathakrishnan's [1] earlier work was compared with the current work. The base pressure effect for the same Mach Number, NPR, and area ratio is shown in Figure 8 from Pandey and Rathakrishnan [1]. The study's L/D ratio was adjusted between 2 and 10 for validation.

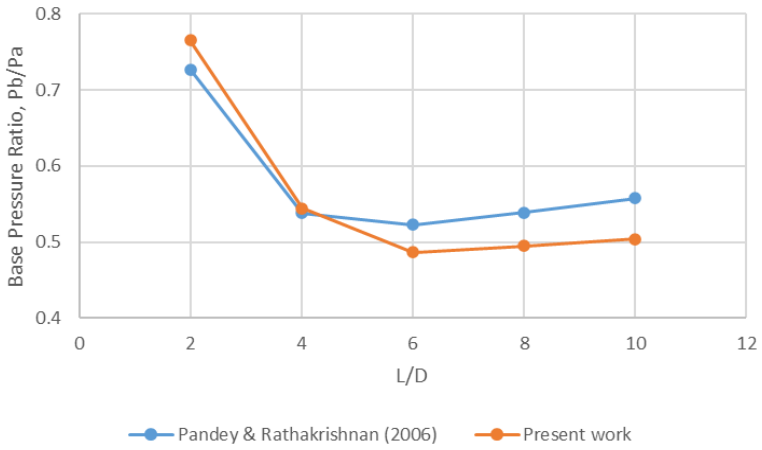

Fig. 8. Present study verification

Figure 8 displays consistent patterns with minimal error margin indicating successful validation as the percentage error for all base pressure ratios at different L/D is less than 10%.

In this paper, The results of this experiment are divided into 2 groups which vary in the NPR and the location of the cavity. This is to achieve both objectives of this experiment which is to know the optimum location and dimension of the cavity in regulating the base pressure to reduce the base drag.

4.2 Calculation Procedure

Continuity, momentum, and energy equations govern the CFD to analyze the flow of base pressure. It starts with the volume flow rate for incompressible flow at each cross-section of a stream tube.

$$\dot{Q} = AV \tag{1}$$

where A = cross-section of the stream tube, V = velocity of the flowing fluid.

However, the mass flow rate of incompressible flow is constant throughout. Given,

$$\dot{m} = \rho AV \tag{2}$$

where, ρ = density of the fluid.

The article of Zuraidi *et al.,* [6] says that for compressible ideal gas flow, the full set of governing equations in terms of continuity, momentum, and energy can be expressed as follows, where the parameters with a bar represent the time-averaged values.

$$\frac{\delta}{\delta \mathrm{t}}+\frac{\delta}{\delta \mathrm{x_i}}\left(\bar{\rho}\tilde{u}_{\mathrm{i}}\right)=0 \tag{3}$$

The term M_X is the turbulence generation given by Eq. (8), the turbulent Prandtl number is σ_k, turbulent kinetic energy dissipation rate is represented by ε.

$$M_X=\mu_t{}'\left(\frac{\partial u_{a,i}}{\partial x_{a,j}}+\frac{\partial u_{a,j}}{\partial x_{a,i}}\right)\frac{\partial u_{\,a,i}}{\partial x_{a,j}}-\frac{2}{3}K\delta_{ij}\frac{\partial u_{a,i}}{\partial x_{a,j}} \tag{4}$$

The kinetic energy of turbulence dissipation (i.e., ε-equation) is given by

$$\frac{\partial(\rho_a u_a \varepsilon)}{\partial z_d}+\frac{1}{r_d}\frac{\partial(\rho_a v_a \varepsilon)}{\partial r_d}=\frac{\partial}{\partial z_d}\left[\left(\mu'+\frac{\mu_t{}'}{\sigma_\varepsilon}\right)\frac{\partial \varepsilon}{\partial z_d}\right]+\frac{1}{r_d}\frac{\partial}{\partial r_d}\left[r_d\left(\mu'+\frac{\mu_t{}'}{\sigma_\varepsilon}\right)\frac{\partial \varepsilon}{\partial r_d}\right]-\overline{C_1}\overline{f_1}\left(\frac{\varepsilon}{k_a}\right)M_X-\overline{C_2}\overline{f_2}\left(\frac{\varepsilon^2}{k_a}\right) \tag{5}$$

where $\mu_t{}'=\rho_a\overline{f_\mu}\,\overline{C_\mu}\,{k_a}^2/\varepsilon$ denotes turbulent viscosity, and the arbitrary constants are denoted as

$\overline{C_\mu}$, $\overline{C_1}$, $\overline{C_2}$, $\overline{f_\mu}$, σ_k, and σ_ε .

4.3 Base Pressure Variation with L/D

In this part, the results of the base pressure ratio at three NPRs are presented. The NPRs 5, 10.7, and 13 indicate over-expansion, correct expansion, and under-expansion. The Mach number is set at 2.2 and the fixed duct's diameter is used at 22 mm. The L/D is varied from 1, 2, 4, and 6 hence the length of the duct used is changing. The NPRs range from 3, 5, 7, 9, 10.7, 13, and 16, and only three NPRs are discussed for the variation with L/D as mentioned above. Figure 9(a) and Figure 9(b) depict the base pressure ratio fluctuations for NPR = 5 at cavity positions of 0.5D and 1D, respectively. The control positioned at 0.5D is unable to impact the flow field because the flow is still overexpanded even at NPR= 5. However, when the cavity is set at 1D, there is a little rise in the base pressure for L/D = 3 and above. Since ambient pressure affects the duct flow field at lower L/Ds, specifically L/D = 1 to 3, flow attachment to the duct wall may not occur. This could be the cause of passive control's lack of effectiveness.

When the flow from the nozzles has correctly expanded the results of the base pressure as a function of L/D for NPR = 10.7 for cavity locations 0.5D and 1D are shown in Figure 9(c) and Figure 9(d). It is well known that when the nozzles are correctly expanded Mach waves will be formed at the nozzle exit and under these conditions when passive control is employed they are marginally effective for cavity location of 0.5D and the control effectiveness improves when the cavity is placed at 1D. The improvement attainment for the cavity located at 1D is attributed to the reattachment length and the minimum duct length needed for the flow to remain attached to the duct wall.

Likewise, when the nozzle flows were simulated for NPR = 13, the jets experienced a favorable pressure gradient. Figure 9 shows the base pressure values for two locations of the cavities at 0.5D and 1D. In this case, too, the control effectiveness is considerable when passive control is located at 1D.

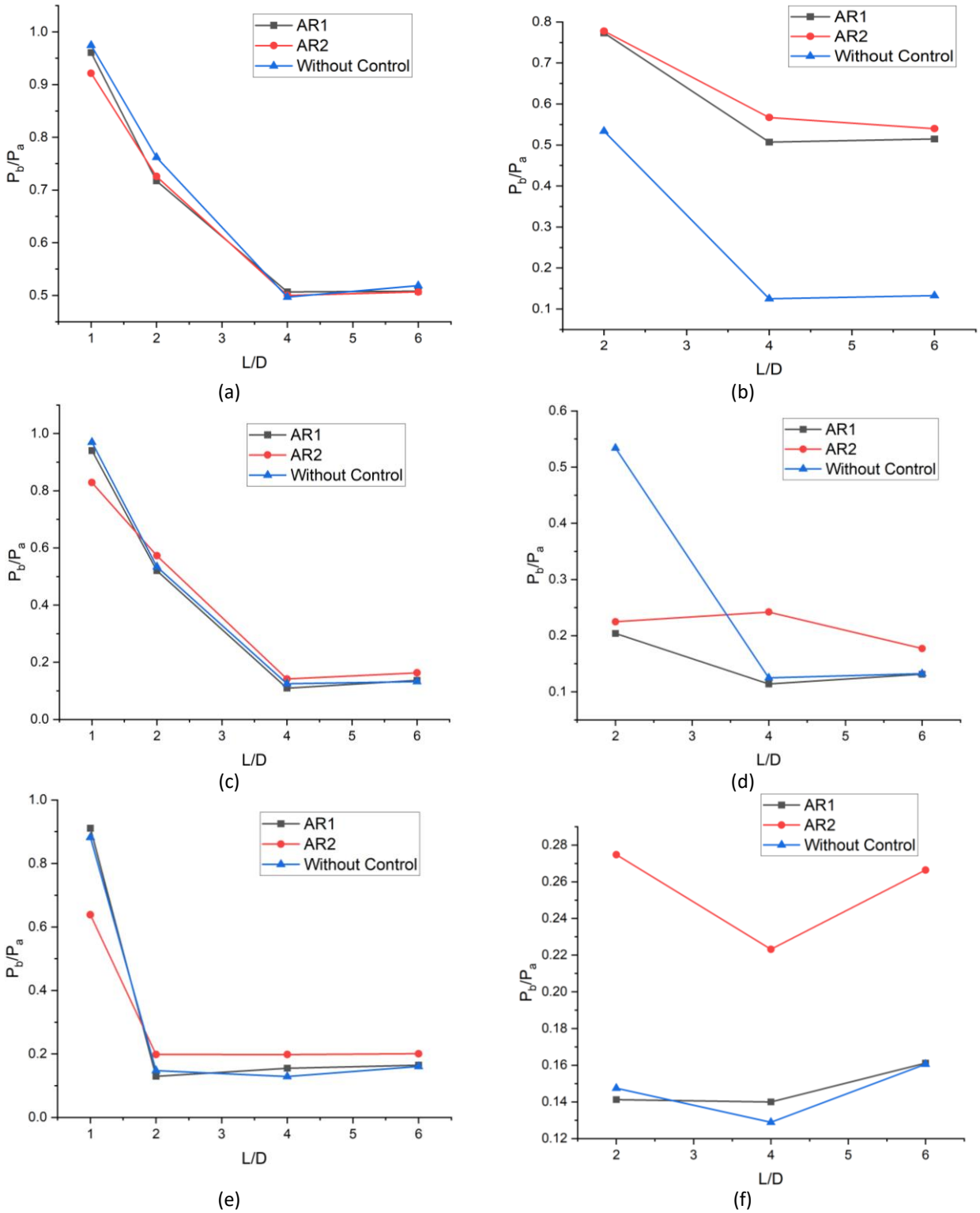

Fig. 9. Base pressure ratio variation with L/D for with and without control duct; (a) NPR 5, 0.5D, (b) NPR 5, 1D, (c) NPR 10.7, 0.5D, (d) NPR 10.7, 1D, (e) NPR 13, 0.5D, (f) NPR 13, 1D

4.4 Base Pressure Variation with Nozzle Pressure Ratio (NPR)

Figure 10(a) shows the results of base pressure for duct length L = 1D for cavity location at 0.5D. Since the duct length is equal to the diameter of the enlarged duct. It looks like the flow is not attached to the wall of the duct. The flow field inside the duct is influenced by the backpressure

resulting in larger values of the base pressure and this trend continues till the jets are over-expanded or perfectly expanded. When the jets are under-expanded there is a decrease in the base pressure for plain duct as well as for duct with cavity AR1. When a cavity with AR2 is employed their control results in further decrement in the base pressure.

Figure 10(b) and (c) show the results of base pressure as a function of NPR when the duct length is 2D and the control is located at 0.5D and 1D. Since NPR for correct expansion is 10.7 the decreasing trend in base pressure continues even though flow from the nozzle is under-expanded. The physics behind this trend may be due to the large duct diameter the reattachment length will be large as compared to the smaller duct diameter. All the parameters are the same except the location of the cavity is at 1D. Since the cavity is moved downstream there is a strong interaction of the waves within the cavity leading to an increase in the base pressure for the cavity with AR2.

The study examines the effectiveness of control in a 4D Figure 10(d)-(g), duct with cavity placements at 0.5D, 1D, 2D, and 3D. Control effectiveness is marginally effective at 0.5D, with a decreasing trend in base pressure arrest. When control locations are shifted to 1D, the flow field remains unchanged, but the control is highly effective for cavity AR2. Control effectiveness is not significant for cavities with an AR1 aspect ratio, but AR2 is most effective, resulting in increased base pressure. The 3D cavity location is optimum due to its distance and small reattachment length, indicating that the control effectiveness may be marginalized.

When the duct length is 6D, Figure 10(h)-(l) show base pressure as a function of NPR for various cavity locations at 0.5D, 1D, 2D, 3D, and 4D. When the cavity is placed at 0.5D the control with AR2 is effective and results in an increase of the base pressure and the cavity with AR1 is not effective as the flow does not see the presence of the cavity. However, when the cavity length is 6 mm due to interactions of the shear layer the control is effective. When the passive control is placed at a 1D location there is further improvement in the control efficacy. As discussed earlier cavity with AR1 is not effective but the cavity with AR2 is effective. Similar results are seen when cavities are located in 2D, 3D, and 4D.

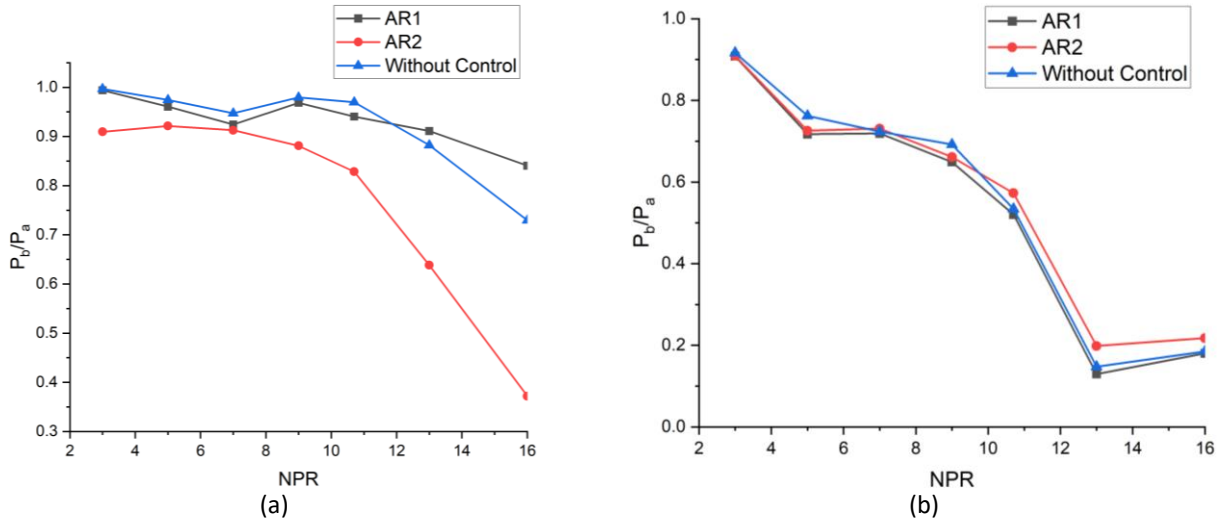

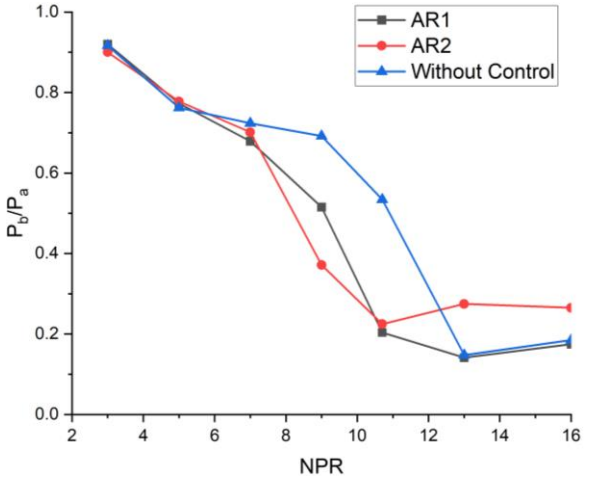
AR1
AR2
Without Control
P_b/P_a
NPR

(c)

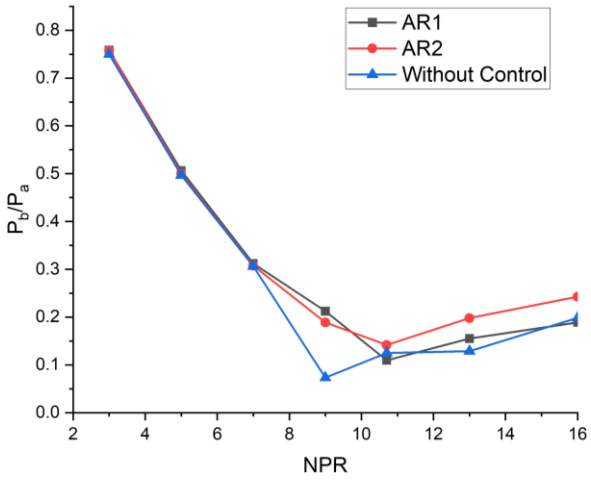
AR1
AR2
Without Control
P_b/P_a
NPR

(d)

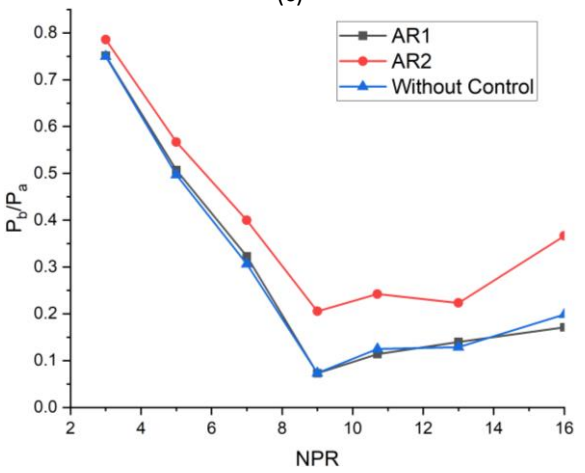
AR1
AR2
Without Control
P_b/P_a
NPR

(e)

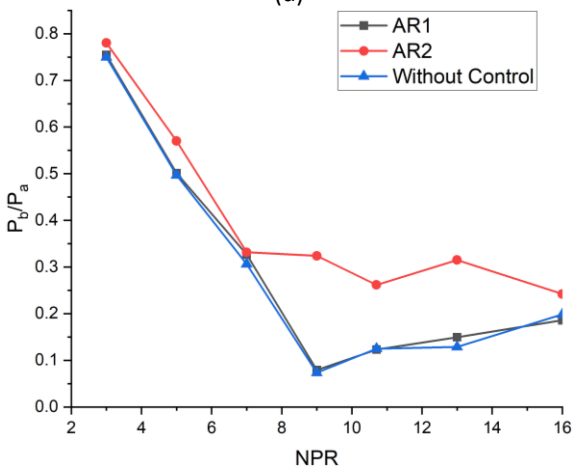
AR1
AR2
Without Control
P_b/P_a
NPR

(f)

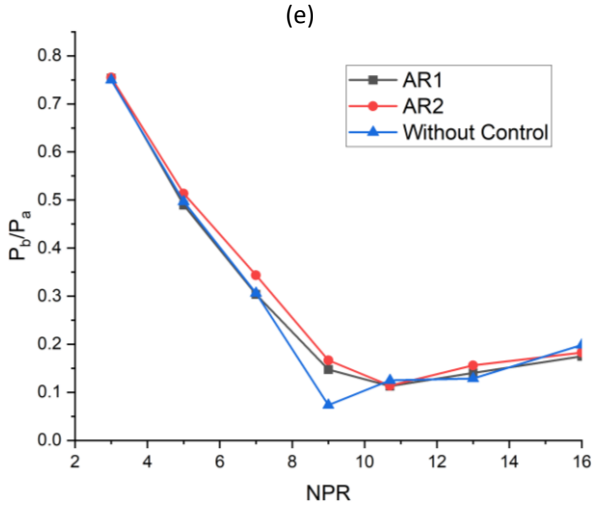
AR1
AR2
Without Control
P_b/P_a
NPR

(g)

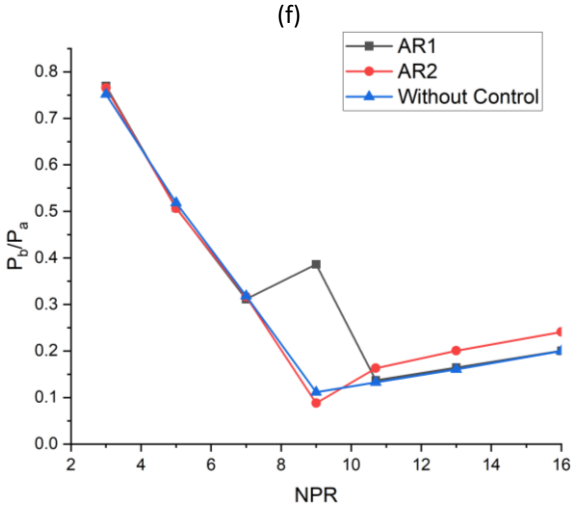
AR1
AR2
Without Control
P_b/P_a
NPR

(h)

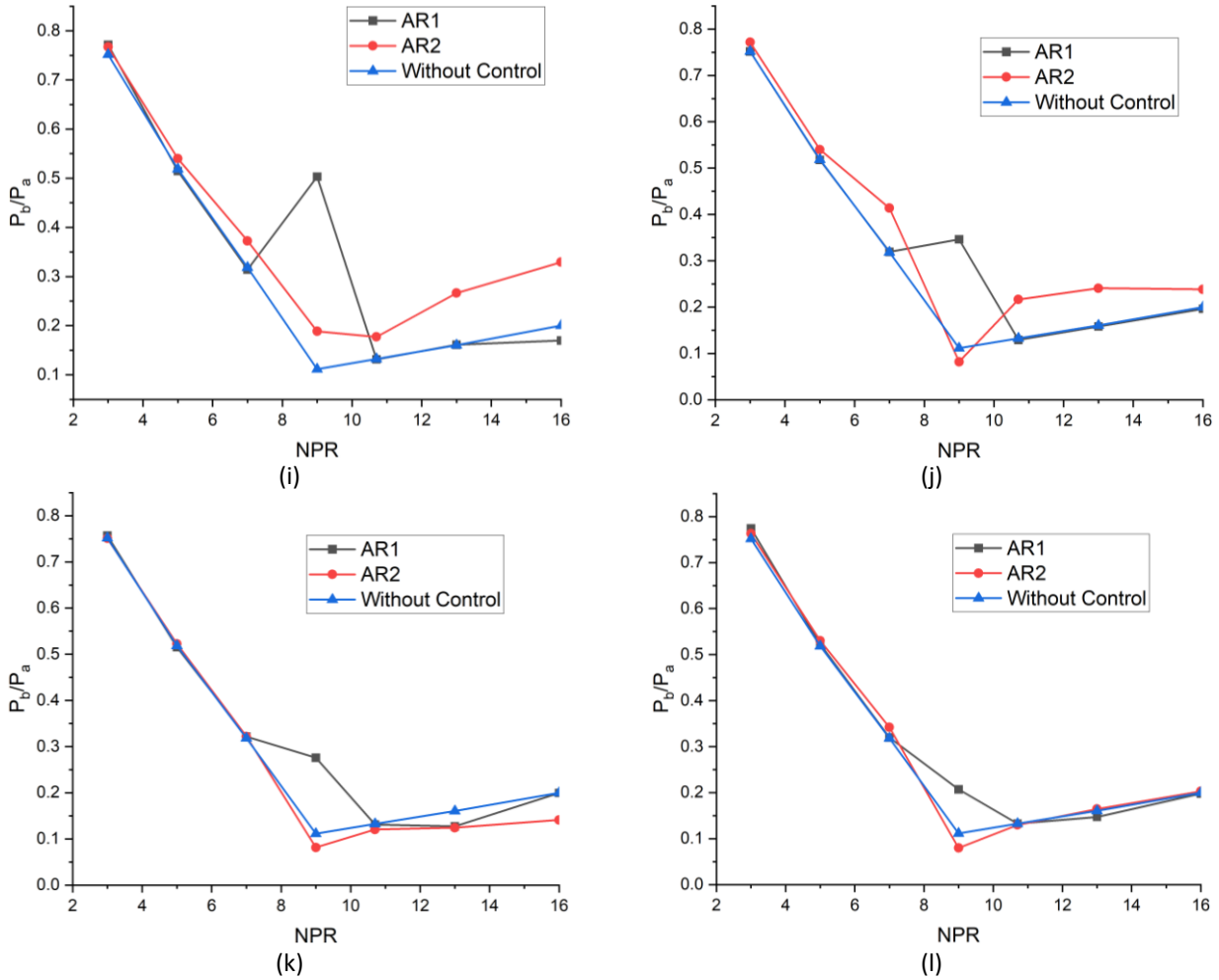

Fig. 10. Base pressure ratio variation with NPR for with and without control duct; (a) L/D 1, 0.5D, (b) L/D 2, 0.5D, (c) L/D 2, 1D, (d) L/D 4, 0.5D, (e) L/D 4, 1D, (f) L/D 4, 2D, (g) L/D 4, 3D, (h) L/D 6, 0.5D, (i) L/D 6, 1D, (j) L/D 6, 2D, (k) L/D 6, 3D, (l) L/D 6, 4D

4.5 Pressure contours for Cavity at the 3D Location for L/D 6

From Figure 11, it is evident for L/D 6 that when the cavity is placed near the reattachment point i.e. 3D for the over-expanded cases the oblique shock waves are formed at the nozzle exit. Whereas for the correctly expanded Figure 11(c) and under-expanded cases (Figure 11(d) and (e)) the bow shock and expansion waves are formed. Here cavity acts as a closed cavity hence, its presence cannot be observed.

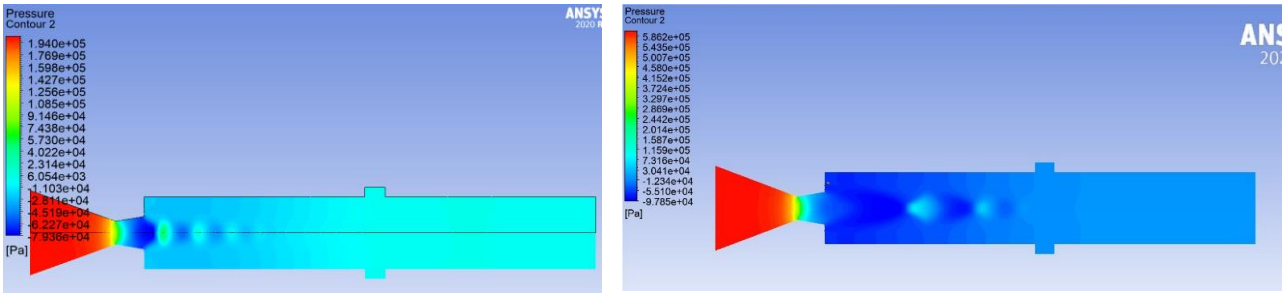

(a) NPR 3 (b) NPR 7

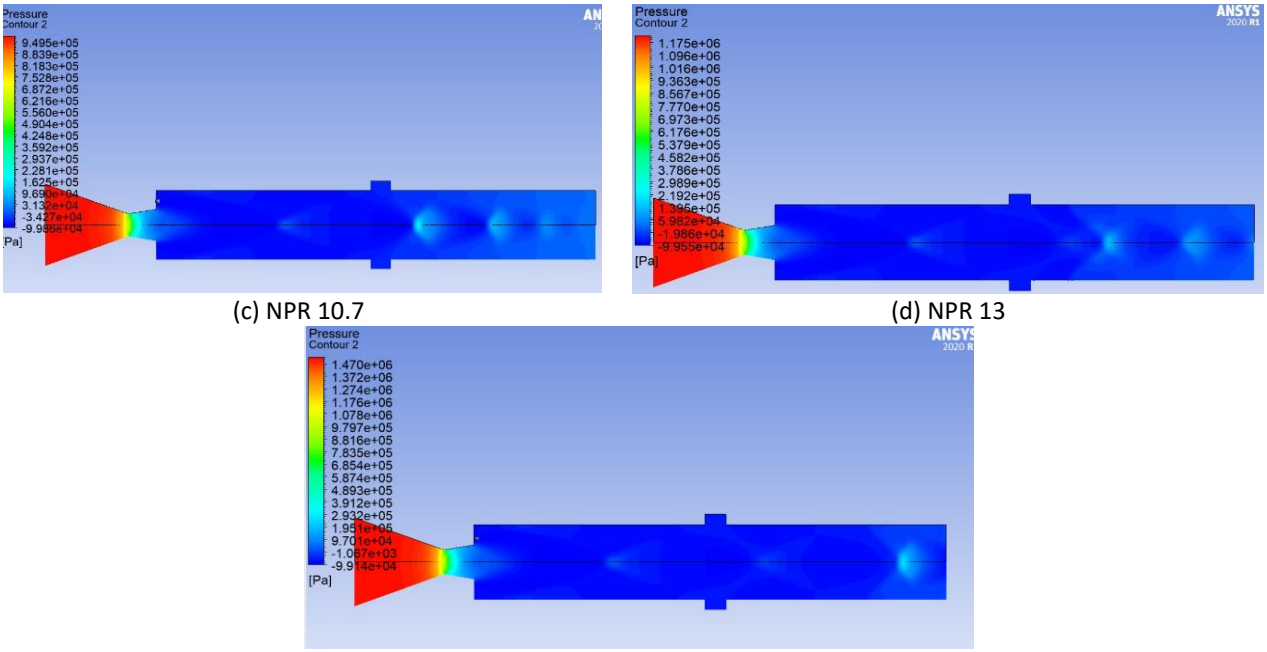

(c) NPR 10.7 (d) NPR 13

(e) NPR 16

Fig. 11. Pressure contour with control for cavity location at 3D for duct length L = 6D

4.6 Pressure Contours without Control for L/D 6

Here in Figure 12, similar results are observed in the pressure for without control case.

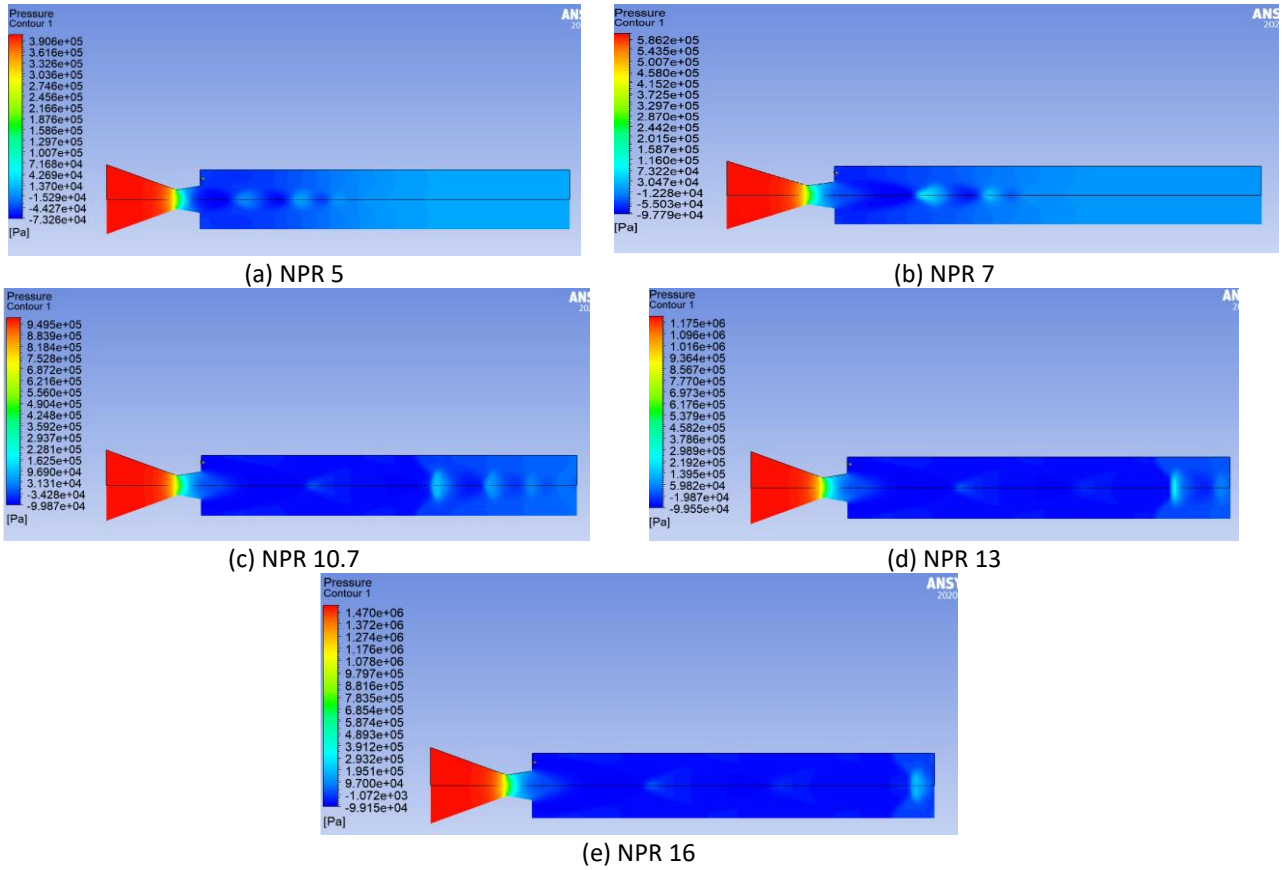

(a) NPR 5 (b) NPR 7

(c) NPR 10.7 (d) NPR 13

(e) NPR 16

Fig. 12. Pressure contour without control for cavity location at 3D for duct length L = 6D

5. Conclusion

As a result of the above discussions, the investigation into base pressure regulation utilizing a cavity has yielded insightful information and possible answers for enhancing aerodynamic performance in a variety of technical applications. To improve stability, maneuverability, and fuel efficiency, it is feasible to alter the flow characteristics and reduce drag by using a cavity at the base of a vehicle or building. Compared to a plain duct, the presence of a cavity in a duct significantly affects the base pressure for aspect ratio AR2 at 0.5D as compared to the other locations.

References

[1] Pandey, K. M., and E. Rathakrishnan. "Annular cavities for Base flow control." *International Journal of Turbo and Jet Engines* 23, no. 2 (2006): 113-128. https://doi.org/10.1515/TJJ.2006.23.2.113

[2] Sethuraman, Vigneshvaran, Parvathy Rajendran, and Sher Afghan Khan. "Base and wall pressure control using cavities and ribs in a suddenly expanded flows-an overview." *Journal of Advanced Research in Fluid Mechanics and Thermal Sciences* 66, no. 1 (2020): 120-134.

[3] Rathakrishnan, E. "Effect of ribs on suddenly expanded flows." *AIAA Journal* 39, no. 7 (2001): 1402-1404. https://doi.org/10.2514/2.1461

[4] Viswanath, P. R. "Drag reduction of afterbodies by controlled separated flows." *AIAA Journal* 39, no. 1 (2001): 73-78. https://doi.org/10.2514/2.1272

[5] Aabid, Abdul, Azmil Afifi, Fharukh Ahmed Ghasi Mehaboob Ali, Mohammad Nishat Akhtar, and Sher Afghan Khan. "CFD analysis of splitter plate on the bluff body." *CFD Letters* 11, no. 11 (2019): 25-38.

[6] Zuraidi, Nur Husnina Muhamad, Sher Afghan Khan, Abdul Aabid, Muneer Baig, and Istiyaq Mudassir Shaiq. "Passive Control of Base Pressure in a Converging-Diverging Nozzle with Area Ratio 2.56 at Mach 1.8." *Fluid Dynamics & Materials Processing* 19, no. 3 (2023). https://doi.org/10.32604/fdmp.2023.023246

[7] Khan, Ambareen, Nurul Musfirah Mazlan, Mohd Azmi Ismail, and Mohammad Nishat Akhtar. "Experimental and numerical simulations at sonic and supersonic Mach numbers for area ratio 7.84." *CFD Letters* 11, no. 5 (2019): 50-60.

[8] Hirst, Trevor, Chuanpeng Li, Yunchao Yang, Eric Brands, and Gecheng Zha. "Bluff body drag reduction using passive flow control of jet boat tail." *SAE International Journal of Commercial Vehicles* 8, no. 2015-01-2891 (2015): 713-721. https://doi.org/10.4271/2015-01-2891

[9] Milićev, Snežana S., Miloš D. Pavlović, Slavica Ristić, and Aleksandar Vitić. "On the influence of spike shape at supersonic flow past blunt bodies." *Facta Universitatis-Series: Mechanics, Automatic Control and Robotics* 3, no. 12 (2002): 371-382.

[10] Khan, Ambareen, Nurul Musfirah Mazlan, and Mohd Azmi Ismail. "Analysis of flow through a convergent nozzle at Sonic Mach Number for Area Ratio 4." *Journal of Advanced Research in Fluid Mechanics and Thermal Sciences* 62, no. 1 (2019): 66-79.

[11] Khan, Ambareen, Parvathy Rajendran, Junior Sarjit Singh Sidhu, S. Thanigaiarasu, Vijayanandh Raja, and Qasem Al-Mdallal. "Convolutional neural network modeling and response surface analysis of compressible flow at sonic and supersonic Mach numbers." *Alexandria Engineering Journal* 65 (2023): 997-1029. https://doi.org/10.1016/j.aej.2022.10.006

[12] Khan, Sher Afghan, Mohammed Asadullah, and Jafar Sadhiq. "Passive control of base drag employing dimple in subsonic suddenly expanded flow." *International Journal of Mechanical & Mechatronics Engineering IJMME-IJENS* 18, no. 03 (2018): 69-74.

[13] Khan, Sher Afghan, Mohammed Asadullah, G. M. Fharukh Ahmed, Ahmed Jalaluddeen, and Maughal Ahmed Ali Baig. "Passive control of base drag in compressible subsonic flow using multiple cavities." *International Journal of Mechanical and Production Engineering Research and Development* 8, no. 4 (2018): 39-44. https://doi.org/10.24247/ijmperdaug20185

[14] Azami, Muhammed Hanafi, Mohammed Faheem, Abdul Aabid, Imran Mokashi, and Sher Afghan Khan. "Experimental research of wall pressure distribution and effect of micro jet at Mach." *International Journal of Recent Technology and Engineering* 8, no. 2S3 (2019): 1000-1003. https://doi.org/10.35940/ijrte.B1187.0782S319

[15] Khan, Sher Afghan, Abdul Aabid, and C. Ahamed Saleel. "Influence of micro-jets on the flow development in the enlarged duct at supersonic Mach number." *International Journal of Mechanical and Mechatronics Engineering* 19, no. 01 (2019): 70-82.

[16] Azami, Muhammed Hanafi, Mohammed Faheem, Abdul Aabid, Imran Mokashi, and Sher Afghan Khan. "Inspection of supersonic flows in a CD nozzle using experimental method." *International Journal of Recent Technology and Engineering* 8, no. 2S3 (2019): 996-999. https://doi.org/10.35940/ijrte.B1186.0782S319

[17] Aabid, Abdul, and Sher Afghan Khan. "Investigation of high-speed flow control from CD nozzle using design of experiments and CFD methods." *Arabian Journal for Science and Engineering* 46, no. 3 (2021): 2201-2230. https://doi.org/10.1007/s13369-020-05042-z

[18] Sajali, Muhammad Fahmi Mohd, Abdul Aabid, Sher Afghan Khan, Fharukh Ahmed Ghasi Mehaboobali, and Erwin Sulaeman. "Numerical investigation of the flow field of a non-circular cylinder." *CFD Letters* 11, no. 5 (2021): 37-49.

[19] Pathan, Khizar Ahmed, Prakash S. Dabeer, and Sher Afghan Khan. "Investigation of base pressure variations in internal and external suddenly expanded flows using CFD analysis." *CFD Letters* 11, no. 4 (2019): 32-40.

[20] Pathan, Khizar Ahmed, Prakash S. Dabeer, and Sher Afghan Khan. "Effect of nozzle pressure ratio and control jet location to control base pressure in suddenly expanded flows." *Journal of Applied Fluid Mechanics* 12, no. 4 (2019): 1127-1135. https://doi.org/10.29252/jafm.12.04.29495

[21] Fharukh, Ahmed G. M., Mohammad Asad Ullah, and Sher Afghan Khan. "Experimental study of suddenly expanded flow from correctly expanded nozzles." *ARPN Journal of Engineering and Applied Sciences* 11, no. 16 (2016): 10041-10047.

[22] Akhtar, Mohammad Nishat, Elmi Abu Bakar, Abdul Aabid, and Sher Afghan Khan. "Control of CD nozzle flow using microjets at Mach 2.1." *International Journal of Innovative Technology and Exploring Engineering (IJITEE)* 8, no. 9S2 (2019): 631-635. https://doi.org/10.35940/ijitee.I1128.0789S219

[23] Shamitha, Shamitha, Asha Crasta, Khizar Ahmed Pathan, and Sher Afghan Khan. "Analytical and Numerical Simulation of Surface Pressure of an Oscillating Wedge at Hypersonic Mach Numbers and Application of Taguchi's Method." *Journal of Advanced Research in Applied Sciences and Engineering Technology* 30, no. 1 (2023): 15-30. https://doi.org/10.37934/araset.30.1.1530

[24] Pathan, Khizar Ahmed, Prakash S. Dabeer, and Sher Afghan Khan. "Influence of expansion level on base pressure and reattachment length." *CFD Letters* 11, no. 5 (2019): 22-36.

[25] Pathan, Khizar Ahmed, Syed Ashfaq, Prakash S. Dabeer, and Sher Afgan Khan. "Analysis of parameters affecting thrust and base pressure in suddenly expanded flow from nozzle." *Journal of Advanced Research in Fluid Mechanics and Thermal Sciences* 64, no. 1 (2019): 1-18.

[26] Shaikh, Sohel Khalil, Khizar Ahmed Pathan, Zakir Ilahi Chaudhary, B. G. Marlpalle, and Sher Afghan Khan. "An Investigation of Three-Way Catalytic Converter for Various Inlet Cone Angles Using CFD." *CFD Letters* 12, no. 9 (2020): 76-90. https://doi.org/10.37934/cfdl.12.9.7690

[27] Shaikh, Sohel Khalil, Khizar Ahmed Pathan, Zakir Ilahi Chaudhary, and Sher Afghan Khan. "CFD analysis of an automobile catalytic converter to obtain flow uniformity and to minimize pressure drop across the monolith." *CFD Letters* 12, no. 9 (2020): 116-128. https://doi.org/10.37934/cfdl.12.9.116128